NASA/GSFC SCANNING RAMAN LIDAR MEASUREMENTS OF WATER VAPOR AND CLOUDS DURING IHOP

David N. Whiteman[1], Belay Demoz[1], Paolo Di Girolamo[2], Joe Comer[3], Zhien Wang[4], Rei-Fong Lin[4], Keith Evans[4], Igor Veselovskii[4]

[1]NASA/Goddard Space Flight Center, Greenbelt, Maryland, david.n.whiteman@nasa.gov
[2]University of Basillicata, Potenza, Italy
[3]Science Systems Applications, Inc, Lanham, Maryland
[4]University of Maryland, Baltimore County, Baltimore, Maryland

ABSTRACT

The NASA/GSFC Scanning Raman Lidar (SRL) participated in the International H_2O Project (IHOP) that occurred in May and June, 2002 in the midwestern part of the U. S. The SRL acquired measurements of water vapor, aerosols, cloud liquid and ice water, and temperature for more than 200 hours during IHOP. Here we report on the SRL water vapor and cirrus cloud measurements with particular emphasis being given to the measurements of June 19-20, 2002, which are motivating cirrus cloud model comparison studies.

1. INTRODUCTION

The International H_2O Project (IHOP - http://www.atd.ucar.edu/dir_off/projects/2002/IHOP.html) was the largest meteorological field campaign ever held in the United States. Its goal was to measure convective storm systems with sufficient detail to permit quantitative precipitation forecasting to be improved. IHOP included participants from numerous U.S. and foreign government agencies as well as universities. The instrumentation used during IHOP included seven research aircraft carrying three water vapor lidars and one wind lidar, mobile radar systems for storm-chasing, and a ground-based site in the western panhandle of Oklahoma that included the NASA/GSFC SRL, GLOW molecular wind lidar [1], and HARLIE [2] scanning aerosol lidar. Other instrumentation at Homestead were Vaisala and SnowWhite radiosonde systems [3], cloud and aerosol radar, AERI (Atmospheric Emitted Radiance Interferometer), SuomiNet GPS (http://www.unidata.ucar.edu/ suominet/) and an AERONET (http://aeronet.gsfc.nasa.gov/) sun photometer.

2. THE SCANNING RAMAN LIDAR (SRL)

The SRL was deployed to IHOP with a substantially new optical configuration that provided measurements of water vapor mixing ratio, aerosol backscatter, extinction and depolarization, cloud liquid [4] and ice water [5], and rotational Raman temperature [6]. This new optical configuration used two telescopes: a 0.76m F/5.2 Dall-Kirkham for high altitude measurements and a 0.25m F/2.5 Newtonian for the low altitude Raman measurements, accomplished via fiber optic coupling, and for aerosol depolarization measurements using traditional optics. The laser used was a Continuum tripled Nd:YAG (354.7 nm) operating at 30 Hz and generating approximately 9 W of output power. The fields of view of the large and small telescopes were approximately 0.25 and 1.2 mrad, respectively. The narrow field of view of the large telescope coupled with narrow spectral filters in the water vapor and nitrogen channels (2.5A and 2.8A, respectively) and the combined use of analog and photon counting data acquisition permitted the full intensity water vapor and nitrogen signals to be sensed throughout the diurnal cycle. This enabled the water vapor mixing ratio to be quantified during the daytime at significantly higher temporal and spatial resolution than was previously possible.

3. DATA ANALYSIS

3.1 Water vapor mixing ratio

Water vapor mixing ratio is calculated from the ratio of the water vapor and nitrogen Raman channels of the SRL [7,8]. Differential transmission is calculated using atmospheric density from radiosonde and the measured aerosol extinction from the lidar. The water vapor mixing ratio measurements were calibrated by comparing the integral of the lidar mixing ratio profile with the total precipitable water derived from SuomiNet GPS. Due to the differences in sampling volumes between GPS and lidar, a mean SRL calibration value derived from daily comparisons between SRL and GPS was used to recalibrate the entire SRL dataset. The final SRL water vapor calibration was derived from an updated set of GPS retrievals that used a forecast model to improve the conversion of atmospheric path delays measured at various angles to a vertical measurement of total precipitable water. These newer SuomiNet retrievals are on average approximately 3% drier than the ones that were available in near-real time during the IHOP experiment. An overlap correction of up to 8% was

applied to the SRL water vapor mixing ratio data in the lowest 1 km to account for slight differences between the overlap functions of the water vapor and nitrogen channels. In addition, and for the first time, the temperature dependence of narrowband water vapor and N_2 Raman measurements were accounted for in the analysis of the mixing ratio data [7,8]. This effect leads to an apparent moistening of the mid- and upper-tropospheric (UT) water vapor mixing ratio measurements due primarily to a shift of intensity in the Raman spectrum of water vapor toward the band origin as temperatures decrease, as is typical with increasing altitude in the troposphere. For the optical configuration of the SRL during the IHOP campaign, the magnitude of this effect in th UT was approximately 10%. The details of the calculation of this correction, which are based on 1 cm^{-1} resolution measurements of the water vapor and nitrogen channel transmissions using a Nicolet 870 Fourier Transform Spectrometer, will be provided at the conference.

3.2 Cirrus cloud optical depth and extinction to backscatter ratio

Cloud boundaries are determined using a scattering ratio threshold of 2.0. These boundaries are then used in the calculation of cirrus cloud optical depth where the upper reference altitude is chosen several km above the top of the cloud to minimize the influence of multiple scattering on the determination of optical depth [9]. The integrated backscatter is determined by integrating the profile of cloud backscatter coefficient, which has been shown to be essentially insensitive to multiple scattering. [10]. The layer mean extinction to backscatter ratio (S) is then given by the ratio of the optical depth and the integrated backscatter coefficient. Multiple scattering studies have been performed [11] to minimize the errors in the calculation of cirrus cloud optical depth.

4. WATER VAPOR RANDOM ERROR CHARACTERIZATION

The random error in the water vapor mixing ratio measurement was quantified using the measurements of May 22, 2003 shown in Fig. 1.

Fig. 1 presents the water vapor mixing ratio displayed over an altitude range of 0.3 – 5.0 km and for more than 6 hours, a period that was characterized by a growing boundary layer (BL) that collapsed at dusk (~25 UT in the image, this mean 0100 UT on May 23) as the dryline influenced the local water vapor environment more strongly. Vertical plumes of water vapor can be seen in Fig. 1 from 21.5 to beyond 24.0 UT. These are updraft regions that gave rise to convective clouds as the day progressed. These convective clouds can be seen as white features at the top of the BL in the aerosol scattering ratio image shown in Fig. 2. For more details on this case, see

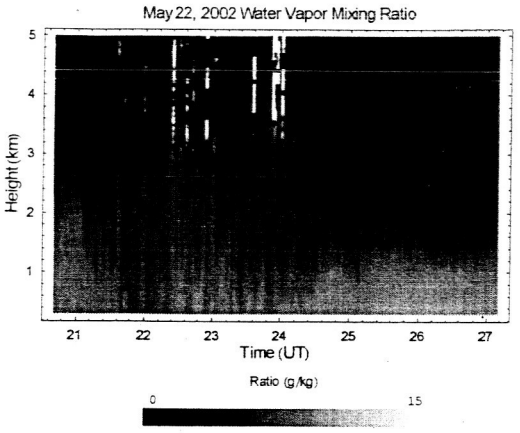

Fig. 1 Water vapor mixing ratio measured on May 22, 2002 during IHOP during the passage of a dryline neat the lidar site.

reference [12].

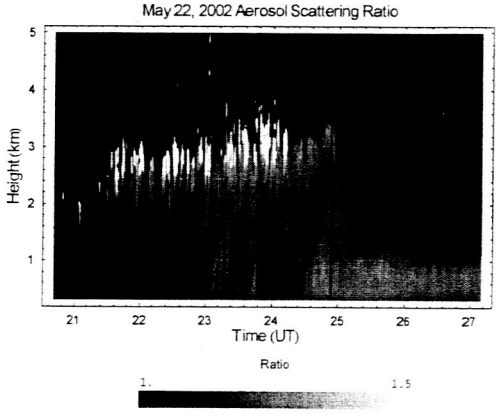

Fig. 2 the aerosol scattering ratio image corresponding to the water vapor image shown in Fig. 1.

The water vapor mixing ratio measurements shown in Fig. 1 possess approximately 2 minute temporal and between 60-200 meter spatial resolution as determined by the half-power point in the Fourier spectrum.

Using this resolution, the random error was calculated at three times in the dataset shown in Fig. 1: 21, 23, 26.5 UT. (The latter time indicates 0230 on May 23, 2002). The first two of these times were in bright daytime conditions while the last was in full darkness. The random error of the water vapor mixing ratio measurements for

these three times are shown in Fig. 3.

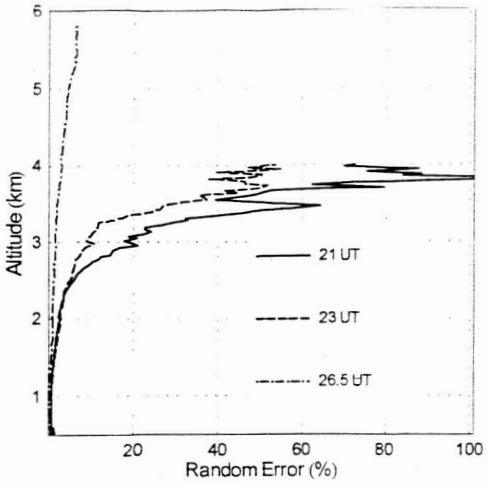

Fig. 3 Random error in the SRL water vapor mixing ratio measurements on May 22, 2002.

These random error quantifications indicate that under all conditions, the random error in the mixing ratio measurement remains below 10% throughout the boundary layer at 2 minute temporal and 60 - 200 meter spatial resolution. During the daytime, the random errors increase steeply above the boundary layer where the water vapor content drops rapidly. However, under nighttime conditions, the random error does not exceed 10% below ~6 km. These high-resolution water vapor measurements permit boundary layer convective processes to be studied throughout the diurnal cycle as further described in reference [12].

5. JUNE 19-20, 2002 BORE AND CIRRUS CLOUD EVENT

Because of the importance of atmospheric wave activity to the inititiation of convection, buoyancy oscillations, also known as bores, were a focus of IHOP. An extended set of SRL measurements acquired on June 19-20, 2002 revealed the atmosphere to possess a rich set of waves in the water vapor field as shown in the bottom of Fig. 4. At approximately 0630 UT on June 20, as indicated by the base of the arrow, the strongest bore event observed during the measurement period occurred. The oscillations in the moisture field at ~3.5 km are likely due to the upward thrust of energy from below. The overlying cirrus cloud field, created by anvil outflow from a thunderstorm to the north, is also shown in the upper part of the figure.

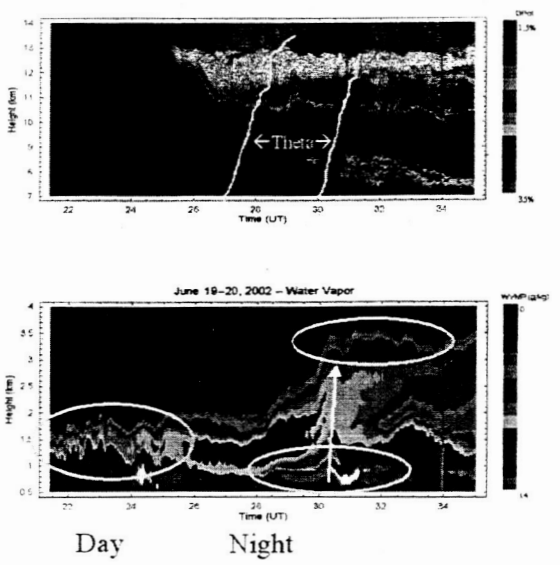

Day Night

Fig. 4 Water vapor (lower panel) and cirrus cloud (upper panel) fields on June 19-20 during IHOP with prominent waves circled. The major bore event is shown with an arrow. The vertical structure of the potential temperature from radiosonde reveals well-mixed regions in the upper levels of the cirrus clouds.

The oscillations in the lower cirrus layer seen in the upper image of the figure are suggestive of the possibility that energy from this bore event at ~0.5km in altitude has propagated upward to ~9km and induced the oscillations in this cirrus layer. This possibility has been studied by calculating the Scorer parameter, which considers the balance between the atmospheric stability and wind shear as a function of altitude. These results are shown in Fig. 5 based on SRL water vapor measurements and radiosonde wind measurements made every 2 hours. The increase in the Scorer parameter above approximately 4 km does not support the hypothesis that upward wave energy could have been responsible for the oscillations in the lower cirrus layer. However, further analysis will be done using the higher temporal resolution GLOW [1] molecular wind measurements in an effort to see if there as a period during which upward propagation of energy may have

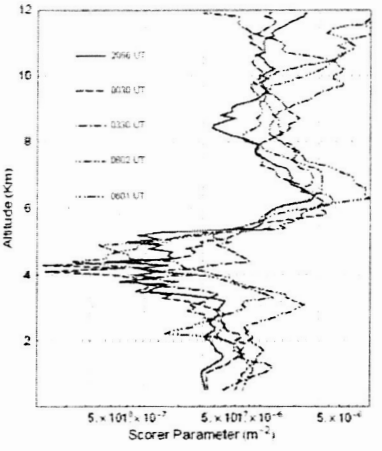

Fig. 5 Scorer parameter calculations for June 19-20, 2002

been possible that the radiosonde wind measurements did not capture.

6. CIRRUS CLOUD MODELING

The cirrus cloud measurements of June 19-20 provide some of the most detailed remote measurements of an evolving cirrus cloud field every captured. The SRL was able to measure water vapor mixing ratio, cirrus optical depth and extinction to backscatter ratio, depolarization, ice water content, generalized particle radius [5] and temperature [6,13]. Through the use of multiple scattering calculations [11], we expect to be able to calculate the profile of extinction and S in this cloud. This large body of measurements, along with radiosonde data such as the potential temperature profile shown in Fig. 5, is being used as input to a cirrus cloud model maintained at NASA/GSFC [14]. Preliminary model predictions for the June 19-20 case are shown in Fig. 6.

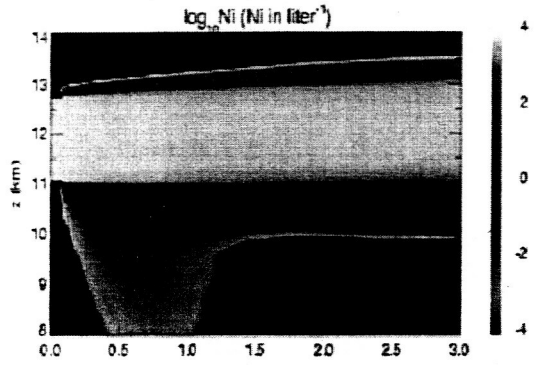

Fig. 6 Model simulations of ice particle density based on inputs from the June 19-20 cirrus case measured by the SRL.

These first model simulations of ice particle number density over a period of three hours indicate light precipitation from the cirrus cloud early in the simulation period, which began at 0400 UT on June 20. Further model comparisons will be performed and shown at the conference using the additional lidar derived information that is now available. But these initial simulations imply that the nuclei for the formation of the lower cirrus layer may have been provided by light precipitation from the upper cirrus layer making these cirrus cloud measurements potentially an example of a "seeder-feeder" cloud system. No such precipitation is evident in the lidar data, however, so this precipitation would have to have been very light indeed. We will study the threshold for detection of light cirrus precipitation from the SRL and compare this with further model simulations to study this possibility.

7. SUMMARY

The NASA/GSFC participated in the first International H_2O Project in May-June 2002. A new configuration of the SRL enabled measurements of water vapor, aerosol backscatter, extinction, depolarization, liquid water, ice water and temperature. The daytime water vapor measurements were greatly improved over previous configurations of the instrument. This measurement capability has been used here to study an interesting bore/cirrus cloud case from June 19-20 during IHOP. Strong oscillations in the lower moisture field are correlated with oscillations in the cirrus cloud field at 9km. The possibility that these lower oscillations were induced by an upward thrust of energy from near the surface is being studied. The SRL measurements of this cirrus cloud case are also motivating cirrus cloud model studies with the goal of using the extensive measurements available for the June 19-20 case as a validation dataset for cirrus model development.

REFERENCES

1. Gentry, B et. al., GLOW Measurements during IHOP. This conference.
2. Schwemmer, et. al., HARLIE Measurements during IHOP. This conference.
3. Wang, J, et. al., Performance of operational radiosonde humidity sensors in direct comparison with a chilled mirror dew-point hygrometer and its climate implication Geophys. Res. Lett., 30, 16, 1860, 2003.
4. Russo, F., et. al., Development of Raman Lidar Techniques to address the Aerosol Indirect Effect: The Liquid Water Content of CloudsThis conference.
5. Wang, Z., et. al., Raman Lidar Ice Water Measurement. This conference.
6. Di Girolamo, P., et. al. Rotational Raman Lidar measurements of atmospheric temperature in the UV Geophys. Res. Lett., **31**, L01106, 2004.
7. Whiteman, D. N. Examination of the traditional Raman lidar technique. II. Evaluating the ratios for water vapor and aerosols *Appl. Opt.*, 42, No. 15, 2593-2608, 2003b
8. Whiteman, D. N., Examination of the traditional Raman lidar technique. I. Evaluating the temperature-dependent lidar equations *Appl. Opt*, 42, No. 15, 2571-2592, 2003a
9. Whiteman, D. N., et. al., Raman lidar measurements of water vapor and cirrus clouds during the passage of hurricane Bonnie *J. of Geophys. Res.*, 106, No. D6, 5211-5225, 2001.
10. Wandinger, Experimental determination of the lidar overlap profile with Raman lidar *Appl. Opt.*, 37, No. 3, 417-427, 1998.
11. Gambacorta, A., et. al., Cirrus Cloud Particle Size Retrievals Using Multiple Scattering. This conference.
12. Demoz, B et. al., Analysis of a Dryline Case from IHOP. This conference.
13. Marchese, R., et.al., SRL Temperature Retrievals from IHOP. This conference
14. Lin, R-F, et. al., , Cirrus Parcel Model Comparison Project. Phase 1: The critical components to simulate cirrus initiation explicitly J. Atmos. Sci., 59, 15, 2305-2329, 2002